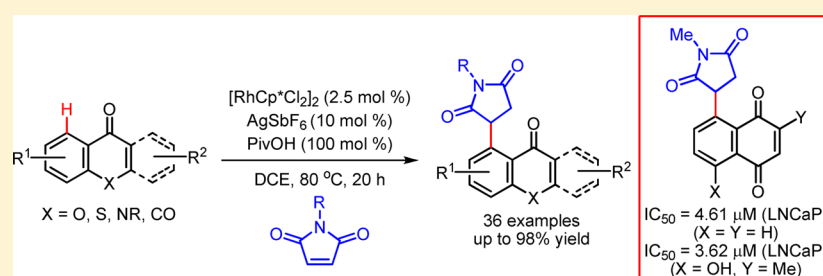


Synthesis of Succinimide-Containing Chromones, Naphthoquinones, and Xanthenes under Rh(III) Catalysis: Evaluation of Anticancer Activity

Sang Hoon Han,[†] Saegun Kim,[†] Umasankar De, Neeraj Kumar Mishra, Jihye Park, Satyashel Sharma, Jong Hwan Kwak,[‡] Sangil Han, Hyung Sik Kim,^{*} and In Su Kim^{*,‡}

School of Pharmacy, Sungkyunkwan University, Suwon 16419, Republic of Korea

Supporting Information



ABSTRACT: The weakly coordinating ketone group directed C–H functionalizations of chromones, 1,4-naphthoquinones, and xanthenes with various maleimides under rhodium(III) catalysis are described. These protocols efficiently provide a range of succinimide-containing chromones, naphthoquinones, and xanthenes with excellent site selectivity and functional group compatibility. All synthetic compounds were screened for in vitro anticancer activity against human breast adenocarcinoma cell lines (MCF-7). In particular, compounds **7aa** and **7ca** with a naphthoquinone scaffold were found to be highly cytotoxic, with an activity competitive with anticancer agent doxorubicin.

INTRODUCTION

The ketone-containing bi- and tricyclic scaffolds have been recognized as ubiquitous frameworks found in a large number of chromones,¹ naphthoquinones,² and xanthenes.³ In particular, this class of compounds has attracted considerable attention by virtue of their diverse and interesting biological activities, i.e., anticancer activity, antioxidant activity, α -glucosidase inhibitory activity, antibacterial activity, and antifungal activity (Figure 1).⁴ In fact, the biological properties of these molecules are closely related with conjugated bi- and

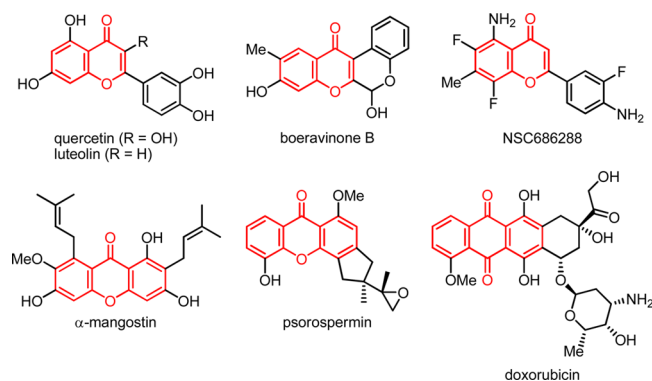


Figure 1. Representative and biologically relevant chromones, naphthoquinones, and xanthenes.

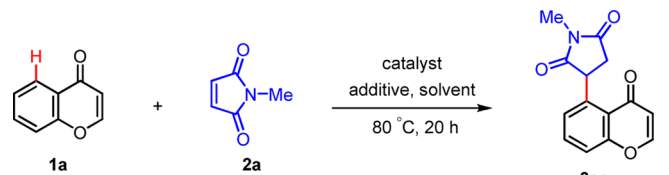
tricyclic motifs with the ketone functionality, but vary depending on the nature, position, and variant of substituents. As a consequence, various synthetic derivatives have been synthesized and evaluated for clinical applications.

The past decade witnessed the development of atom and step economical process for the construction of complex molecular architectures from simple feedstocks. In this regard, the transition metal-catalyzed C–H functionalization has been established as a pivotal strategy for the efficient production of structurally diverse molecules in organic and medicinal chemistry.⁵ In this area, much effort has been devoted to the catalytic C–H functionalization of compounds containing a ketone moiety as a directing group.⁶ In particular, the ketone-assisted site-selective C–H functionalization of chromones⁷ and quinones⁸ has been of intensive research area due to the prevalence of many pharmaceutical agents.

Recently, maleimides have been widely used in the direct functionalization events of C(sp²)–H and C(sp³)–H bonds under transition-metal catalysis to afford the corresponding succinimides.⁹ In this context, succinimides can be generated via olefin insertion to the metallacycle intermediate followed by a subsequent protonation pathway.^{9a–c} Generally, succinimides have been known as privileged structural units found in many bioactive compounds and functional materials, thus making

Received: October 25, 2016

Published: November 22, 2016

Table 1. Selected Optimization of Reaction Conditions^a


entry	catalyst (mol %)	additive (mol %)	solvent	yield ^b (%)
1	[RhCp*Cl ₂] ₂ (2.5)	AgSbF ₆ (10), PivOH (200)	DCE	99
2	[RhCp*Cl ₂] ₂ (2.5)	AgSbF ₆ (10)	DCE	10
3	[RhCp*Cl ₂] ₂ (2.5)	PivOH (200)	DCE	NR
4		AgSbF ₆ (10), PivOH (200)	DCE	NR
5	[Ru(<i>p</i> -cymene)Cl ₂] ₂ (2.5)	AgSbF ₆ (10), PivOH (200)	DCE	19
6	[CoCp*(CO)I ₂] (5)	AgSbF ₆ (10), PivOH (200)	DCE	trace
7	[RhCp*Cl ₂] ₂ (2.5)	AgSbF ₆ (10), AcOH (200)	DCE	94
8	[RhCp*Cl ₂] ₂ (2.5)	AgSbF ₆ (10), NaOAc (200)	DCE	9
9	[RhCp*Cl ₂] ₂ (2.5)	AgSbF ₆ (10), Cu(OAc) ₂ (200)	DCE	64
10	[RhCp*Cl ₂] ₂ (2.5)	AgSbF ₆ (10), AgOAc (200)	DCE	24
11	[RhCp*Cl ₂] ₂ (2.5)	AgSbF ₆ (10), PivOH (200)	MeOH	75
12	[RhCp*Cl ₂] ₂ (2.5)	AgSbF ₆ (10), PivOH (200)	CH ₂ Cl ₂	53
13	[RhCp*Cl ₂] ₂ (2.5)	AgSbF ₆ (10), PivOH (200)	THF	56
14	[RhCp*Cl ₂] ₂ (2.5)	AgSbF ₆ (10), PivOH (200)	toluene	N.R.
15	[RhCp*Cl ₂] ₂ (2.5)	AgSbF ₆ (10), PivOH (100)	DCE	95
16	[RhCp*Cl ₂] ₂ (2.5)	AgSbF ₆ (10), PivOH (50)	DCE	71
17 ^c	[RhCp*Cl ₂] ₂ (2.5)	AgSbF ₆ (10), PivOH (100)	DCE	75

^aReaction conditions: **1a** (0.2 mmol), **2a** (0.4 mmol, 2 equiv), catalyst (quantity noted), additive (quantity noted), solvent (1 mL) under air at 80 °C for 20 h in pressure tubes. ^bYield by flash column chromatography. ^c**2a** (0.24 mmol, 1.2 equiv) was used.

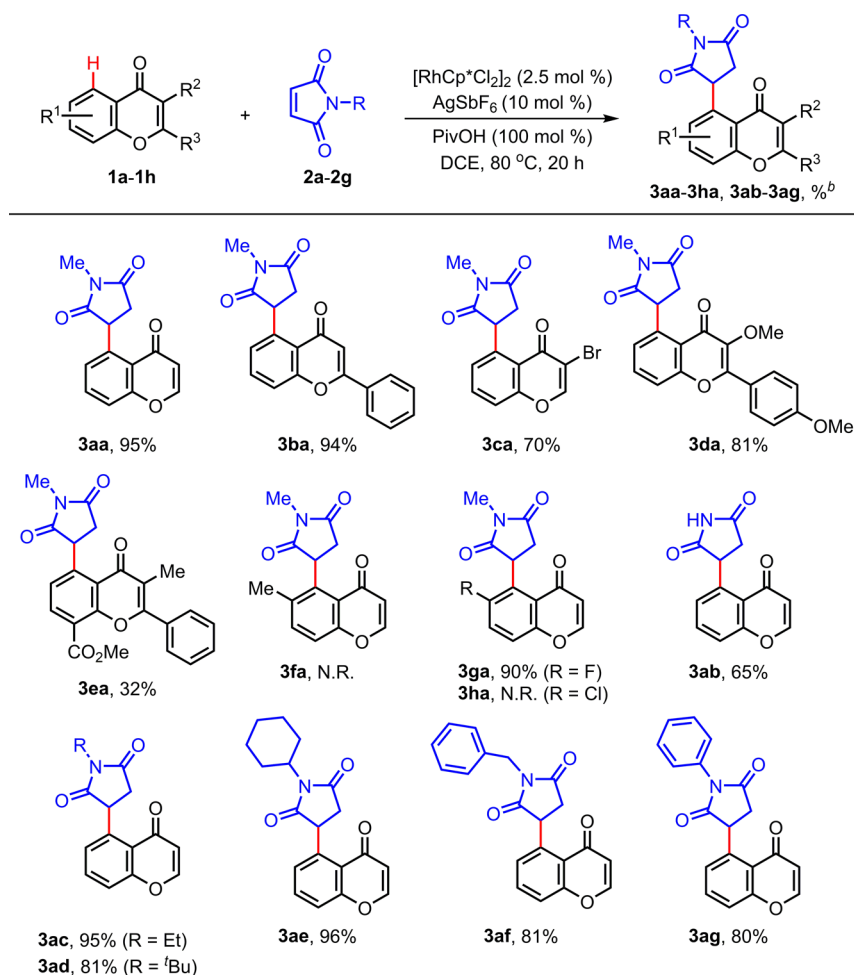
them one of the most promising scaffolds in drug discovery.¹⁰ In continuation of our efforts toward the development of new anticancer agents based on the catalytic C–H functionalization of bioactive scaffolds using various coupling partners,¹¹ we herein report the rhodium(III)-catalyzed C–H alkylation of chromones, naphthoquinones, and xanthenes with maleimides affording various succinimide derivatives. In addition, all synthetic compounds have been screened for cytotoxic activity against human breast adenocarcinoma MCF-7 cell lines. Moreover, compounds selected from initial activity screening were further tested against various cancer cell lines, such as human prostate adenocarcinoma cells (LNCaP), human liver carcinoma cells (HepG2), human lung carcinoma cells (A549), and human ovarian carcinoma cells (SKOV3), and were found to exhibit promising anticancer properties competitive with anticancer doxorubicin. For mechanistic understanding of the anticancer activity of synthetic compounds, the ROS generation experiment of our synthetic compounds and ROS inhibition experiment using *N*-acetyl-L-cysteine (NAC) as a radical scavenger were also performed.

RESULTS AND DISCUSSION

Our optimization was initiated by examining the reaction of 4*H*-chromen-4-one (**1a**) and *N*-methylmaleimide (**2a**) under our previous reported conditions, as shown in entry 1 of Table 1.^{9c,d} Gratifyingly, the coupling reaction between **1a** and **2a** under cationic Rh(III) catalysis in the presence of pivalic acid (PivOH) additive were observed to afford the desired product **3aa** in quantitative yield (Table 1, entry 1). Control experiments revealed that cationic rhodium catalyst and PivOH additive are highly required for this transformation (Table 1, entries 2–4).^{12a} Other catalysts such as Ru(II)^{12b} and Co(III) were found to be less effective in the coupling reaction

(Table 1, entries 5 and 6). Screening of additives and solvents showed that the combination of AgSbF₆ and PivOH in DCE solvent was found to be most effective for this reaction (Table 1, entries 7–14). Interestingly, we were pleased to find that lowering the amount of PivOH to 100 mol % also provided the desired product **3aa** in 95% yield (Table 1, entry 15). The structure of **3aa** was unambiguously determined by X-ray crystallographic analysis (see the Supporting Information). Finally, treatment of either 50 mol % of PivOH (Table 1, entry 16) or 1.2 equiv of **2a** (Table 1, entry 17), respectively, showed the decreased formation of **3aa**.

With the optimal reaction conditions in hand, the substrate scope of chromones with maleimides was investigated, as shown in Table 2. C2- and C3-substituted chromones **1b–d** were found to be good substrates for the coupling reaction with **2a**, affording the C5-succinimide-containing chromones **3ba–da**. However, chromone **1e** with an electron-deficient substituent at the C8-position underwent the cross-coupling reaction in a relatively lower yield under the current reaction conditions. This result suggests that this reaction might proceed with the electrophilic rhodation pathway in the C–H cleavage step. Notably, sterically hindered C6-substituted chromones **1f** and **1h** were found to be unreactive, whereas fluoro-substituted chromone **1g** at the C6-position was found to be a suitable substrate in the coupling reaction to give the corresponding product **3ga** in high yield (90%). Meanwhile, the scope of maleimides was also screened to couple with **1a** under the optimized reaction conditions. To our delight, unprotected maleimide **2b** was found to undergo the alkylation reaction to furnish **3ab** in 65% yield. Additionally, other alkyl- and aryl-substituted maleimides **2c–g** smoothly participated in the C5-alkylation reaction to afford our desired products **3ac–ag** in high yields.

Table 2. Scope of Chromones with Maleimides^a

^aReaction conditions: **1a–h** (0.2 mmol), **2a–g** (0.4 mmol, 2 equiv), $[\text{RhCp}^*\text{Cl}_2]_2$ (2.5 mol %), AgSbF_6 (10 mol %), PivOH (100 mol %), DCE (1 mL) under air at 80 °C for 20 h in pressure tubes. ^bYield by flash column chromatography.

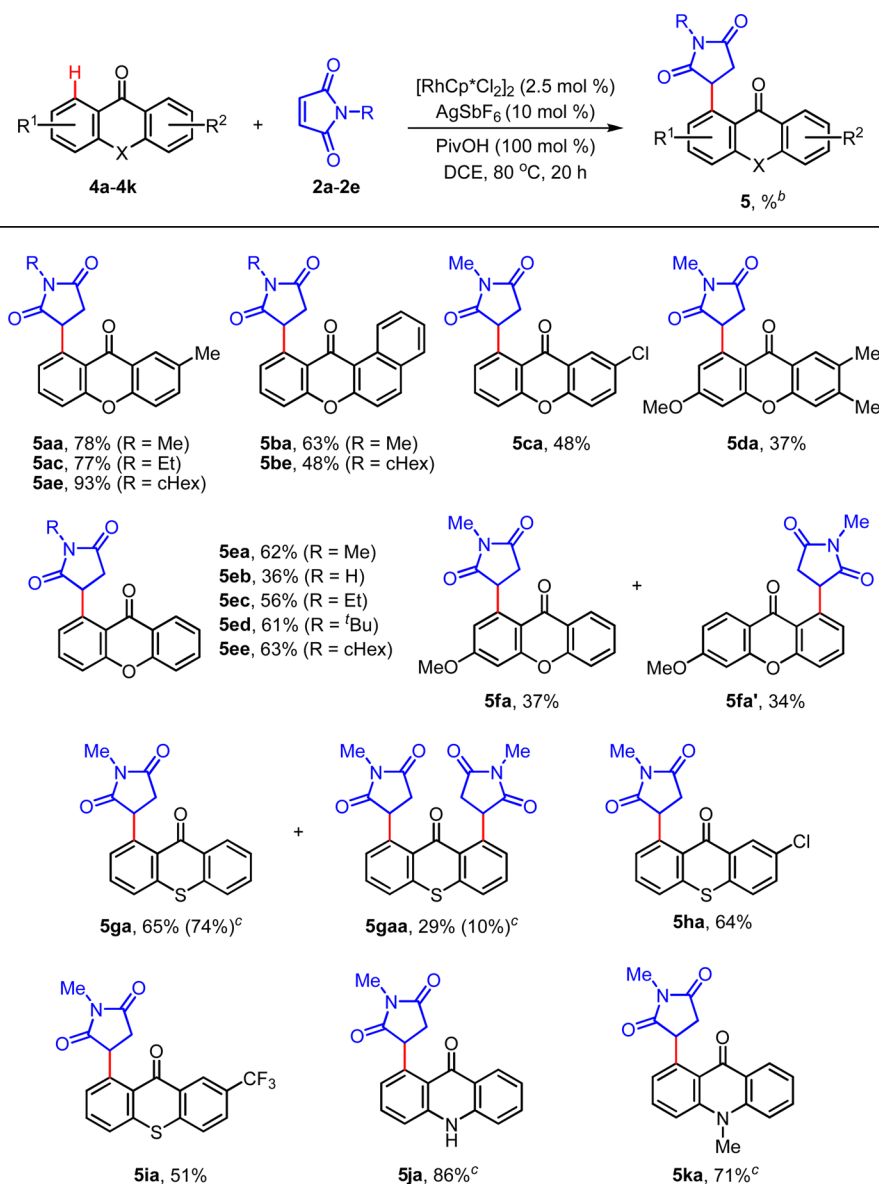
Next, we extended the substrate scope to xanthenes and its analogues such as thioxanthenes and acridinones with various maleimides **2a–e**, as shown in Table 3. The *meta*-substituted xanthenes **4a–d** were found to be coupled with maleimides **2a**, **2c**, and **2e** with complete monoselectivity at the less hindered site providing the corresponding products in 37–93% yields. Interestingly, the reaction of symmetrical xanthone **4e** with maleimides **2a–e** also provided monoalkylated xanthenes **5ea–ee** in 36–63% yields, and a trace amount of bis-alkylated products was observed. Intramolecular competition reaction of **4f** was performed to illustrate the chemoselectivity of this method depending on the electronic properties of aromatic ring. Interestingly, no significant distinction of product distribution between **5fa** and **5fa'** was detected. In sharp contrast, thioxanthone (**4g**) provided a separable mixture of mono- and bis-alkylated products **5ga** and **5gaa** in a ~2:1 ratio in 94% combined yield. To get the high monoselectivity of the product, we further performed the reaction by using a decreased amount of **2a** (120 mol %) and were pleased to see the formation of **5ga** in a satisfactory yield (74%) as a major product. In addition, *meta*-substituted thioxanthenes **4h** and **4i** also underwent the C–H functionalization with **2a** to give the corresponding products **5ha** and **5ia** in moderate yields. Surprisingly, in the case of acridinones **4j** and **4k**, an excellent level of monoselectivity was observed by using 120 mol % of **2a**

under otherwise identical reaction conditions to provide **5ja** and **5ka** in high yields.

Based on the above results, we further screened the site-selective alkylation reaction using 1,4-naphthoquinones and anthraquinone as ketone-containing substrates (Scheme 1). Naphthoquinone (**6a**) was coupled with **2a** to furnish **7aa** in 37% yield. However, naturally occurring lawsone (**6b**) did not deliver the desired product **7ba**, presumably due to the bidentate coordination between ketone and hydroxyl groups to a Rh(III) metal center. To our delight, natural plumbagin (**6c**) was found to be reactive under the standard reaction conditions to afford the succinimide-containing plumbagin derivative **7ca** in 45% yield. Finally, anthraquinone (**6d**) was also found to deliver our desired product **7da** in 32% yield.

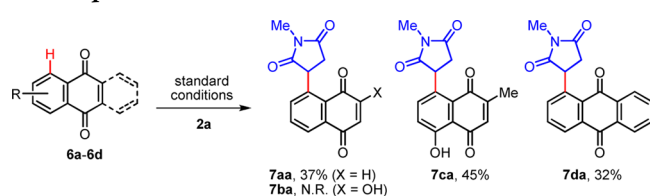
To highlight the robustness and practicality of this transformation, we performed the scale-up experiment of **1a** (5 mmol) using lower catalyst loading (1 mol %) and obtained 1.09 g of **3aa** in 85% yield (Scheme 2).

To gain mechanistic insight, we performed the deuterium-labeling experiment of **1a** with **2a** using AcOD under otherwise identical reaction conditions (Scheme 3). Deuterium incorporation (30%) on the C4-position of succinimide ring and 72% deuterium incorporation of the recovered chromone deuterio-**1a** at the C5-position were detected. The above result indicates

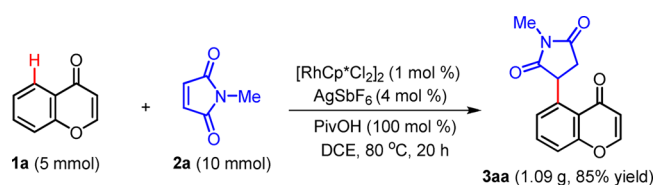
Table 3. Scope of Xanthone Analogues with Maleimides^a

^aReaction conditions: **4a–k** (0.2 mmol), **2a–e** (0.4 mmol, 2 equiv), $[RhCp^*Cl_2]_2$ (2.5 mol %), $AgSbF_6$ (10 mol %), $PivOH$ (100 mol %), DCE (1 mL) under air at 80 °C for 20 h in pressure tubes. ^bYield by flash column chromatography. ^c**2a** (0.24 mmol, 1.2 equiv) was used.

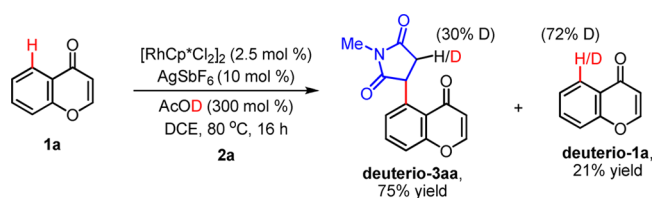
Scheme 1. Reaction of 1,4-Naphthoquinones and Anthraquinone with **2a**



Scheme 2. Scale-up Experiment



Scheme 3. Deuterium-Labeling Experiment



that the initial C–H activation step might be reversible and acid additive can play a role in final protonation step.⁹

All of the synthesized succinimide-containing chromones, naphthoquinones, and xanthones were screened for growth inhibitory activity against human breast adenocarcinoma MCF-7 cell lines, and the results are summarized in Table 4. The MCF-7 cancer cells were exposed for 24 h to increasing concentrations of all compounds, and their survival was determined using the MTT (3-(4,5-dimethylthiazol-2-yl)-2,5-

Table 4. Cytotoxicity of Synthetic Compounds against Human MCF-7 Cancer Cell Lines^a

compd	IC ₅₀ (μM)	compd	IC ₅₀ (μM)	compd	IC ₅₀ (μM)	compd	IC ₅₀ (μM)
3aa	>50	3ae	>50	5da	>50	5gaa	>50
3ba	>50	3af	>50	5ea	>50	5ha	>50
3ca	>50	3ag	>50	5eb	>50	5ia	>50
3da	>50	5aa	>50	5ec	>50	5ja	>50
3ea	>50	5ac	>50	5ed	>50	5ka	>50
3ga	>50	5ae	>50	5ee	41.62	7aa	5.10
3ab	>50	5ba	>50	5fa	>50	7ca	4.91
3ac	>50	5be	>50	5fa'	>50	7da	>50
3ad	>50	5ca	>50	5ga	>50	doxorubicin	5.34

^aIC₅₀ value: substance concentration necessary for 50% inhibition of cell viability.

Table 5. Cytotoxicity of 5ee, 7aa, and 7ca against Various Human Cancer Cell Lines^a

compd	MCF-7 (IC ₅₀ , μM)	LNCaP (IC ₅₀ , μM)	HepG2 (IC ₅₀ , μM)	A549 (IC ₅₀ , μM)	SKOV3 (IC ₅₀ , μM)
5ee	41.62	35.76	65.09	50.67	86.64
7aa	5.10	4.61	11.35	8.92	29.53
7ca	4.91	3.62	7.13	6.11	12.21
doxorubicin	5.34	3.00	4.20	2.98	11.90

^aIC₅₀ value: substance concentration necessary for 50% inhibition of cell viability.

diphenyltetrazolium bromide) assay.¹³ Xanthone derivative **5ee** and naphthoquinone derivatives **7aa** and **7ca** exhibited promising growth inhibition in MCF-7 cells. In particular, succinimide-containing naphthoquinones **7aa** and **7ca** displayed the most potent inhibitory activities (IC₅₀ = 5.10 μM for **7aa**, IC₅₀ = 4.91 μM for **7ca**) among the tested compounds. Thus, compounds **5ee**, **7aa**, and **7ca** were further tested against various cancer cell lines, such as human prostate adenocarcinoma cells (LNCaP), human liver carcinoma cells (HepG2), human lung carcinoma cells (A549), and human ovarian carcinoma cells (SKOV3), as shown in Table 5. In the case of **7aa**, we observed the potent cytotoxicity against LNCaP cell lines, which is comparable to that of the well-known anticancer agent doxorubicin as a positive control.¹⁴ In addition, compound **7ca** showed potent anticancer activity against two cancer cell lines, LNCaP and SKOV3. These results reveal that succinimide-containing naphthoquinone derivatives might be a powerful candidate for anticancer agents.

The reactive oxygen species (ROS) has been known as an essential component for various biological processes in normal cells. However, the excessive production of ROS induces the extinction of cancer cells. A range of anticancer drugs initially induces ROS generation, leading to killing of cancer cells through an apoptotic pathway.¹⁵ Thus, we performed the ROS production experiment using fluorescent CM-H₂DCFDA as a ROS indicator. Generally, CM-H₂DCFDA penetrates into cell cytoplasm, where it is hydrolyzed by intracellular esterase and oxidized by ROS to form 2',7'-dichlorofluorescein (DCF). The resulting fluorescence can be measured by flow cytometry analysis. As shown in Figure 2, our synthetic compounds **7aa** and **7ca** were found to induce an increase of ROS generation, compared to untreated DMSO control, and to generate a lower level of ROS than hydrogen peroxide. However, compound **7da** with no cytotoxic effect against MCF-7 cancer cell lines did not display ROS generation. These results suggest that the ROS generation of succinimide-containing naphthoquinone derivatives may contribute the potent anticancer effect.

To confirm that the cell cytotoxicity is derived from the ROS generation of our synthetic succinimide-containing naphthoquinone derivatives, we carried out the ROS inhibition

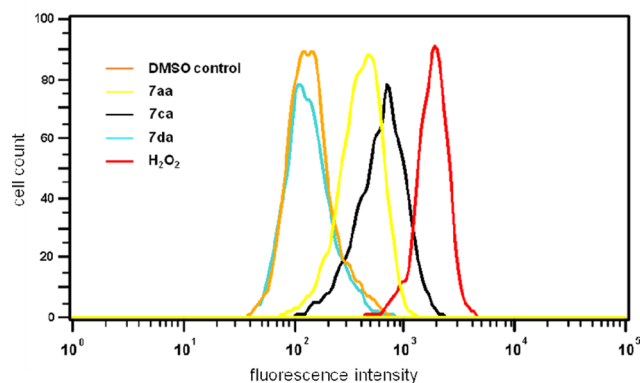


Figure 2. ROS generation experiment of **7aa**, **7ca**, and **7da** in MCF-7 cancer cells.

experiment using *N*-acetyl-L-cysteine (NAC) as a radical scavenger (Figure 3).¹⁶ As shown in Figure 3a, NAC did not show any cytotoxicity up to 5 mM concentration against MCF-7 cancer cell lines. Thus, we pretreated MCF-7 cancer cell lines with NAC in a concentration-dependent manner and observed the cell viability of compound **7ca** at 5 μM concentration (Figure 3b). In the absence of NAC, **7ca** displayed a potent cytotoxic effect. However, as the concentration of NAC increases to 5 mM, the cytotoxicity of **7ca** dramatically decreases. These results indicate that the anticancer effect of our synthetic succinimide-containing naphthoquinone derivatives might be derived from ROS generation.

CONCLUSION

In conclusion, we described the rhodium(III)-catalyzed C–H alkylation reactions of chromones, 1,4-naphthoquinones, and xanthenes with maleimides to afford biologically important succinimide-containing compounds. These transformations have been applied to a wide range of substrates and typically proceed with excellent levels of site-selectivity as well as with high functional group tolerance. All synthesized products were evaluated for anticancer activity against human breast adenocarcinoma MCF-7 cell lines. Compounds **7aa** and **7ca**

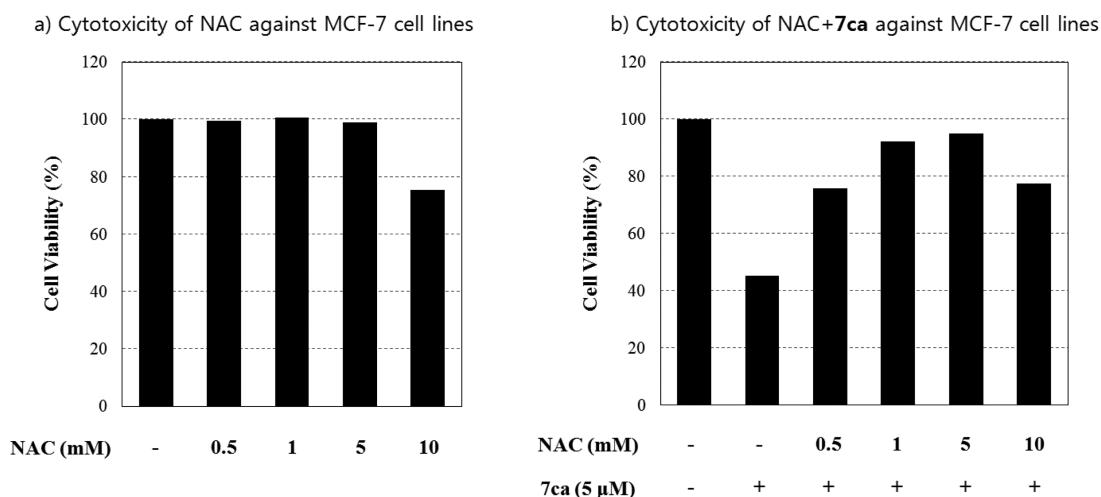


Figure 3. ROS inhibition experiment of 7ca with NAC in MCF-7 cancer cells.

showing a high cytotoxic effect were further screened against other cancer cell lines and were found to exhibit cytotoxic effects competitive with anticancer agent doxorubicin. Further ROS generation experiments indicate that succinimide-containing naphthoquinone derivatives may induce ROS production for potent anticancer effects.

EXPERIMENTAL SECTION

Typical Procedure for the Reaction of Chromones, Naphthoquinones, and Xanthenes with Maleimides. To an oven-dried sealed tube charged with 4H-chromen-4-one (**1a**) (29.2 mg, 0.2 mmol, 100 mol %), [RhCp*Cl₂]₂ (3.1 mg, 0.005 mmol, 2.5 mol %), AgSbF₆ (6.8 mg, 0.02 mmol, 10 mol %), and PivOH (20.4 mg, 0.2 mmol, 100 mol %) were added 1-methyl-1H-pyrrole-2,5-dione (**2a**) (44.4 mg, 0.4 mmol, 200 mol %) and DCE (1 mL) under air at room temperature. The reaction mixture was allowed to stir for 20 h at 80 °C. The reaction mixture was diluted with EtOAc (3 mL) and concentrated in vacuo. The residue was purified by flash column chromatography (EtOAc/*n*-hexanes = 2:1) to afford 48.9 mg of **3aa** in 95% yield.

1-Methyl-3-(4-oxo-4H-chromen-5-yl)pyrrolidine-2,5-dione (3aa): 48.9 mg (95%); white solid; mp = 205.6–208.3 °C; ¹H NMR (400 MHz, DMSO-*d*₆) δ 8.27 (d, *J* = 5.8 Hz, 1H), 7.76 (t, *J* = 7.5 Hz, 1H), 7.66 (d, *J* = 8.1 Hz, 1H), 7.39 (d, *J* = 6.7 Hz, 1H), 6.30 (d, *J* = 5.9 Hz, 1H), 4.42 (br s, 1H), 3.04–2.98 (m, 1H), 2.90 (s, 3H), 2.54 (dd, *J* = 17.3, 6.3 Hz, 1H); ¹³C{¹H} NMR (100 MHz, DMSO-*d*₆) δ 177.7, 177.4, 176.5, 157.7, 156.0, 136.4, 133.7, 130.8, 121.6, 119.1, 113.0, 47.0, 36.9, 24.4; IR (KBr) ν 3080, 2924, 2853, 1774, 1692, 1641, 1603, 1478, 1434, 1340, 1279, 1117, 1029, 770, 687 cm⁻¹; HRMS (orbitrap, ESI) calcd for C₁₄H₁₂NO₄ [M + H]⁺ 258.0766, found 258.0761.

1-Methyl-3-(4-oxo-2-phenyl-4H-chromen-5-yl)pyrrolidine-2,5-dione (3ba): 62.7 mg (94%); light yellow solid; mp = 212.3–215.8 °C; ¹H NMR (500 MHz, DMSO-*d*₆) δ 8.06 (dd, *J* = 7.7, 1.1 Hz, 2H), 7.81–7.76 (m, 2H), 7.62–7.55 (m, 3H), 7.39 (br s, 1H), 6.97 (s, 1H), 4.42 (br s, 1H), 3.03 (br s, 1H), 2.92 (s, 3H), 2.60 (dd, *J* = 17.4, 6.3 Hz, 1H); ¹³C{¹H} NMR (125 MHz, DMSO-*d*₆) δ 178.4, 177.5, 176.6, 161.6, 157.4, 136.2, 133.8, 131.9, 130.8, 130.6, 129.2, 126.3, 120.7, 119.2, 107.6, 47.0, 37.0, 24.5; IR (KBr) ν 3058, 2924, 2856, 1774, 1692, 1632, 1602, 1478, 1435, 1376, 1278, 1118, 1040, 767, 682 cm⁻¹; HRMS (quadrupole, EI) calcd for C₂₀H₁₅NO₄ [M]⁺ 333.1001, found 333.1001.

3-(3-Bromo-4-oxo-4H-chromen-5-yl)-1-methylpyrrolidine-2,5-dione (3ca): 47.1 mg (70%); white solid; mp = 204.1–206.4 °C; ¹H NMR (500 MHz, DMSO-*d*₆) δ 8.88 (s, 1H), 7.82 (t, *J* = 8.1 Hz, 1H), 7.72 (d, *J* = 8.5 Hz, 1H), 7.47 (br s, 1H), 4.48 (br s, 1H), 3.02 (br s, 1H), 2.93 (s, 3H), 2.59 (dd, *J* = 17.4, 6.4 Hz, 1H); ¹³C{¹H} NMR (100 MHz, DMSO-*d*₆) δ 177.4, 176.4, 172.4, 157.4, 154.9, 137.3, 134.2, 131.5, 120.1, 119.3, 110.1, 47.4, 36.7, 24.5; IR (KBr) ν 3056,

2928, 1777, 1697, 1646, 1477, 1438, 1279, 1119, 740, 699 cm⁻¹; HRMS (quadrupole, EI) calcd for C₁₄H₁₀BrNO₄ [M]⁺ 334.9793, found 334.9791.

3-(3-Methoxy-2-(4-methoxyphenyl)-4-oxo-4H-chromen-5-yl)-1-methylpyrrolidine-2,5-dione (3da): 63.9 mg (81%); white solid; mp = 228.9–231.0 °C; ¹H NMR (500 MHz, DMSO-*d*₆) δ 8.07 (d, *J* = 9.0 Hz, 2H), 7.77–7.76 (m, 2H), 7.38 (br s, 1H), 7.14 (d, *J* = 9.1 Hz, 2H), 4.45 (br s, 1H), 3.96 (s, 3H), 3.69 (s, 3H), 3.05 (br s, 1H), 2.94 (s, 3H), 2.65 (dd, *J* = 17.4, 6.3 Hz, 1H); ¹³C{¹H} NMR (125 MHz, DMSO-*d*₆) δ 177.6, 176.6, 174.8, 161.4, 156.3, 156.2, 153.9, 140.3, 136.4, 133.4, 130.2, 130.0, 122.1, 120.9, 119.0, 114.3, 59.3, 55.5, 37.0, 24.5; IR (KBr) ν 2924, 2852, 1770, 1695, 1597, 1436, 1385, 1255, 1177, 1119, 993, 822, 685 cm⁻¹; HRMS (quadrupole, EI) calcd for C₂₂H₁₉NO₆ [M]⁺ 393.1212, found 393.1212.

Methyl 3-Methyl-5-(1-methyl-2,5-dioxopyrrolidin-3-yl)-4-oxo-2-phenyl-4H-chromene-8-carboxylate (3ea): 25.9 mg (32%); white solid; mp = 185.2–187.1 °C; ¹H NMR (400 MHz, DMSO-*d*₆) δ 8.18 (d, *J* = 7.8 Hz, 1H), 7.83–7.81 (m, 2H), 7.61–7.58 (m, 3H), 7.48 (d, *J* = 6.7 Hz, 1H), 4.51 (br s, 1H), 3.88 (s, 3H), 3.03 (br s, 1H), 2.94 (s, 3H), 2.64 (dd, *J* = 17.4, 6.3 Hz, 1H), 2.03 (s, 3H); ¹³C{¹H} NMR (100 MHz, DMSO-*d*₆) δ 178.3, 177.1, 176.5, 164.1, 159.3, 155.1, 141.2, 135.1, 132.1, 130.9, 129.9, 129.2, 128.6, 121.0, 120.0, 117.5, 52.6, 47.5, 36.6, 24.6, 11.5; IR (KBr) ν 3057, 2952, 2849, 1777, 1695, 1622, 1434, 1386, 1277, 1130, 1037, 812, 770, 697 cm⁻¹; HRMS (quadrupole, EI) calcd for C₂₃H₁₉NO₆ [M]⁺ 405.1212, found 405.1209.

3-(6-Fluoro-4-oxo-4H-chromen-5-yl)-1-methylpyrrolidine-2,5-dione (3ga): 49.5 mg (90%); white solid; mp = 216.4–219.7 °C; ¹H NMR (400 MHz, MeOD-*d*₄) δ 8.15 (d, *J* = 5.9 Hz, 1H), 7.73–7.67 (m, 2H), 6.30 (d, *J* = 5.9 Hz, 1H), 4.84–4.80 (m, 1H), 3.11 (dd, *J* = 17.2, 9.1 Hz, 1H), 3.06 (s, 3H), 2.70 (dd, *J* = 17.3, 6.5 Hz, 1H); ¹³C{¹H} NMR (100 MHz, DMSO-*d*₆) δ 177.6 (d, *J*_{C-F} = 2.7 Hz), 177.0, 176.6, 158.0 (d, *J*_{C-F} = 241.5 Hz), 156.4, 155.2 (d, *J*_{C-F} = 218.4 Hz), 122.5 (d, *J*_{C-F} = 2.1 Hz), 122.1 (d, *J*_{C-F} = 28.4 Hz), 121.2 (d, *J*_{C-F} = 13.9 Hz), 121.1 (d, *J*_{C-F} = 9.6 Hz), 112.5, 37.0 (d, *J*_{C-F} = 7.0 Hz), 36.1, 24.5; IR (KBr) ν 3087, 2947, 1775, 1698, 1648, 1468, 1282, 1120, 903, 838, 689 cm⁻¹; HRMS (quadrupole, EI) calcd for C₁₄H₁₀FNO₄ [M]⁺ 275.0594, found 275.0596.

3-(4-Oxo-4H-chromen-5-yl)pyrrolidine-2,5-dione (3ab): 31.6 mg (65%); light yellow solid; mp = 261.1–264.5 °C; ¹H NMR (500 MHz, DMSO-*d*₆) δ 11.05 (br s, 1H), 8.26 (d, *J* = 5.9 Hz, 1H), 7.74 (t, *J* = 7.5 Hz, 1H), 7.63 (d, *J* = 8.4 Hz, 1H), 7.35 (d, *J* = 7.2 Hz, 1H), 6.29 (d, *J* = 5.9 Hz, 1H), 4.42 (br s, 1H), 2.92 (br s, 1H), 2.56 (dd, *J* = 17.3, 6.7 Hz, 1H); ¹³C{¹H} NMR (125 MHz, DMSO-*d*₆) δ 178.6, 177.8, 177.7, 157.6, 155.9, 136.7, 133.7, 130.7, 121.7, 118.9, 113.1, 48.5, 38.2; IR (KBr) ν 3060, 2924, 2856, 1777, 1710, 1648, 1340, 1270, 1178, 741 cm⁻¹; HRMS (orbitrap, ESI) calcd for C₁₃H₁₀NO₄ [M + H]⁺ 244.0609, found 244.0605.

DMSO-*d*₆) δ 8.04 (dd, *J* = 7.6, 1.3 Hz, 1H), 7.85 (t, *J* = 7.6 Hz, 1H), 7.78 (d, *J* = 7.4 Hz, 1H), 7.06 (d, *J* = 10.2 Hz, 1H), 7.01 (d, *J* = 10.2 Hz, 1H), 4.65 (br s, 1H), 3.06 (dd, *J* = 17.5, 9.2 Hz, 1H), 2.94 (s, 3H), 2.64 (dd, *J* = 17.6, 6.2 Hz, 1H); ¹³C{¹H} NMR (100 MHz, DMSO-*d*₆) δ 186.6, 184.7, 177.5, 176.4, 140.1, 137.6, 137.3, 134.1, 133.5, 129.3, 128.9, 126.7, 46.3, 35.8, 24.5; IR (KBr) ν 2925, 2854, 1777, 1698, 1666, 1437, 1289, 1121, 1035, 741, 682 cm⁻¹; HRMS (quadrupole, EI) calcd for C₁₅H₁₁NO₄ [M]⁺ 269.0688, found 269.0685.

3-(4-Hydroxy-7-methyl-5,8-dioxo-5,8-dihydronaphthalen-1-yl)-1-methylpyrrolidine-2,5-dione (7ca): 26.9 mg (45%); brown solid; mp = 195.8–198.6 °C; ¹H NMR (400 MHz, CDCl₃) δ 12.6 (s, 1H), 7.40 (d, *J* = 8.3 Hz, 1H), 7.27 (d, *J* = 6.1 Hz, 1H), 6.81 (s, 1H), 4.21 (br s, 1H), 3.17 (br s, 1H), 3.13 (s, 3H), 2.60 (dd, *J* = 17.5, 5.2 Hz, 1H), 2.12 (s, 3H); ¹³C{¹H} NMR (100 MHz, CDCl₃) δ 190.5, 186.6, 177.6, 176.3, 162.2, 150.4, 138.0, 134.9, 130.2, 129.2, 125.3, 116.3, 46.5, 36.5, 25.2, 16.9; IR (KBr) ν 3631, 3460, 2925, 2360, 2294, 1776, 1694, 1645, 1615, 1435, 1281, 1227, 1119, 957, 794, 623 cm⁻¹; HRMS (quadrupole, EI) calcd for C₁₆H₁₃NO₅ [M]⁺ 299.0794, found 299.0792.

3-(9,10-Dioxo-9,10-dihydroanthracen-1-yl)-1-methylpyrrolidine-2,5-dione (7da): 20.4 mg (32%); light yellow solid; mp = 189.2–191.3 °C; ¹H NMR (400 MHz, CDCl₃) δ 8.42 (d, *J* = 7.8 Hz, 1H), 8.27–8.24 (m, 1H), 8.19–8.17 (m, 1H), 7.80–7.76 (m, 3H), 7.61 (d, *J* = 7.1 Hz, 1H), 4.35 (br s, 1H), 3.24 (br s, 1H), 3.18 (s, 3H), 2.76 (d, *J* = 15.1 Hz, 1H); ¹³C{¹H} NMR (100 MHz, CDCl₃) δ 184.9, 182.9, 177.6, 176.4, 135.9, 134.6, 134.5, 134.4, 134.2, 132.7, 130.9, 128.8, 128.7, 127.8, 127.1, 44.8, 37.1, 25.3; IR (KBr) ν 3653, 2924, 2357, 1698, 1672, 1579, 1435, 1283, 1005, 727, 645 cm⁻¹; HRMS (quadrupole, EI) calcd for C₁₉H₁₃NO₄ [M]⁺ 319.0845, found 319.0820.

Cancer Cell Growth Inhibition Assay (MTT Assay). Human breast adenocarcinoma cells (MCF-7), human prostate adenocarcinoma cells (LNCaP), human liver carcinoma cells (HepG2), human lung carcinoma cells (A549), and human ovarian carcinoma cells (SKOV3) were grown in DMEM medium supplemented with 1% of penicillin/streptomycin and 10% fetal bovine serum (Life Technologies, Grand Island, NY). Cells were seeded in 96-well plates (3 × 10³ cells/well) containing 100 μ L of growth medium for 24 h. After medium removal, 100 μ L of fresh medium containing individual analogue compounds at different concentrations was added to each well and incubated at 37 °C for 48 h. After 24 h of culture, the cells were supplemented with 1 μ L of test compounds dissolved in DMSO (less than 0.025% in each preparation). After 24 h of incubation, 100 μ L of the MTT reagent was added to each well. After 4 h incubation at 37 °C, the supernatant was aspirated, and the formazan crystals were dissolved in 100 μ L of DMSO at 37 °C for 10 min with gentle agitation. The absorbance per well was measured at 540 nm using a VERSA max Microplate Reader (Molecular Devices Corp., USA). The IC₅₀ was defined as the compound concentration required to inhibit cell proliferation by 50% in comparison with cells treated with the maximum amount of DMSO (0.025%) and considered as 100% viability.

Experimental Method for the Detection of ROS Generation.

The formation of intracellular ROS was assayed by the fluorescence emission of 2',7'-dichlorofluorescein diacetate (DCF-DA), which penetrates into the cytoplasm of the cell, where it is hydrolyzed by intracellular esterase and oxidized to form 2',7'-dichlorofluorescein (DCF) by ROS. For the assay, MCF-7 cells were seeded in a covered glass bottom dish at a density of 2 × 10⁴ cells. The MCF-7 cells were pretreated, irradiated, washed twice with Dulbecco's phosphate-buffered saline (DPBS), and loaded with 10 mM DCF-DA solution dissolved in Dulbecco-modified eagle medium (DMEM) (without phenol red) for 30 min at 37 °C in the dark. The cells were subsequently washed twice with DPBS to remove extracellular dye. The quantification of fluorescence intensity was carried out by using a Guava EasyCyte Plus flow cytometer.

■ ASSOCIATED CONTENT

📄 Supporting Information

The Supporting Information is available free of charge on the ACS Publications website at DOI: 10.1021/acs.joc.6b02577.

X-ray crystallographic data for compound 3aa and ¹H and ¹³C NMR spectra of all products (PDF)

X-ray crystallographic data for compound 3aa (CIF)

■ AUTHOR INFORMATION

Corresponding Authors

*Tel: +82-31-290-7789. Fax: +82-31-292-8800. E-mail: hkims@skku.edu.

*Tel: +82-31-290-7788. Fax: +82-31-292-8800. E-mail: insukim@skku.edu.

ORCID

Jong Hwan Kwak: 0000-0002-3731-9539

In Su Kim: 0000-0002-2665-9431

Author Contributions

[†]S.H.H. and S.K. contributed equally.

Notes

The authors declare no competing financial interest.

■ ACKNOWLEDGMENTS

This work was supported by a National Research Foundation of Korea (NRF) grant funded by the Korean government (MSIP) (Nos. 2016R1A4A1011189, 2016R1C1B2010456, and 2015R1A2A1A15053033).

■ REFERENCES

- (a) Sharma, S. K.; Kumar, S.; Chand, K.; Kathuria, A.; Gupta, A.; Jain, R. *Curr. Med. Chem.* **2011**, *18*, 3825. (b) Khadem, S.; Marles, R. J. *Molecules* **2012**, *17*, 191. (c) Gaspar, A.; Matos, M. J.; Garrido, J.; Uriarte, E.; Borges, F. *Chem. Rev.* **2014**, *114*, 4960. (d) Keri, R. S.; Budagumpi, S.; Pai, R. K.; Balakrishna, R. G. *Eur. J. Med. Chem.* **2014**, *78*, 340.
- (a) Sultanbawa, M. U. S. *Tetrahedron* **1980**, *36*, 1465. (b) Pinto, M. M. M.; Sousa, M. E.; Nascimento, M. S. J. *Curr. Med. Chem.* **2005**, *12*, 2517.
- (a) Tandon, V. K.; Kumar, S. *Expert Opin. Ther. Pat.* **2013**, *23*, 1087. (b) Wellington, K. W. *RSC Adv.* **2015**, *5*, 20309.
- (a) Ferry, D. R.; Smith, A.; Malkhandi, J.; Fyfe, D. W.; deTakats, P. G.; Anderson, D.; Baker, J.; Kerr, D. J. *Clin. Cancer Res.* **1996**, *2*, 659. (b) Lin, Y.; Shi, R.; Wang, X.; Shen, H.-M. *Curr. Cancer Drug Targets* **2008**, *8*, 634. (c) Callero, M.; Suárez, G. V.; Luzzani, G.; Itkin, B.; Nguyen, B.; Loaiza-Perez, A. I. *Int. J. Oncol.* **2012**, *41*, 125. (d) Shibata, M.-A.; Iinuma, M.; Morimoto, J.; Kurose, H.; Akamatsu, K.; Okuno, Y.; Akao, Y.; Otsuki, Y. *BMC Med.* **2011**, *9*, 69.
- (5) For recent selected reviews, see: (a) Yang, L.; Huang, H. *Chem. Rev.* **2015**, *115*, 3468. (b) Song, G.; Li, X. *Acc. Chem. Res.* **2015**, *48*, 1007. (c) Li, S.-S.; Qin, L.; Dong, L. *Org. Biomol. Chem.* **2016**, *14*, 4554. (d) Rao, W.-H.; Shi, B.-F. *Org. Chem. Front.* **2016**, *3*, 1028. (e) Sharma, S.; Mishra, N. K.; Shin, Y.; Kim, I. S. *Curr. Org. Chem.* **2015**, *20*, 471.
- (6) (a) Murai, S.; Kakiuchi, F.; Sekine, S.; Tanaka, Y.; Kamatani, A.; Sonoda, M.; Chatani, N. *Nature* **1993**, *366*, 529. (b) Kakiuchi, F.; Murai, S. *Acc. Chem. Res.* **2002**, *35*, 826. (c) Huang, Z.; Lim, H. N.; Mo, F.; Young, M. C.; Dong, G. *Chem. Soc. Rev.* **2015**, *44*, 7764. (d) Zheng, Q.-Z.; Jiao, N. *Tetrahedron Lett.* **2014**, *55*, 1121. (e) Pichette Drapeau, M.; Gooßen, L. J. *Chem. - Eur. J.* **2016**, DOI: 10.1002/chem.201603263. (f) Matsumura, D.; Kitazawa, K.; Terai, S.; Kochi, T.; Ie, Y.; Nitani, M.; Aso, Y.; Kakiuchi, F. *Org. Lett.* **2012**, *14*, 3882.

- (7) (a) Min, M.; Kim, D.; Hong, S. *Chem. Commun.* **2014**, *50*, 8028. (b) Kim, K.; Choe, H.; Jeong, Y.; Lee, J. H.; Hong, S. *Org. Lett.* **2015**, *17*, 2550.
- (8) (a) Fujiwara, Y.; Domingo, V.; Seiple, I. B.; Gianatassio, R.; Del Bel, M.; Baran, P. S. *J. Am. Chem. Soc.* **2011**, *133*, 3292. (b) Ilangovan, A.; Saravanakumar, S.; Malayappasamy, S. *Org. Lett.* **2013**, *15*, 4968. (c) Jardim, G. A. M.; Bower, J. B.; da Silva Júnior, E. N. *Org. Lett.* **2016**, *18*, 4454.
- (9) For the C(sp²)-H functionalization using maleimides, see: (a) Miura, W.; Hirano, K.; Miura, M. *Org. Lett.* **2015**, *17*, 4034. (b) Bettadapur, K. R.; Lanke, V.; Prabhu, K. R. *Org. Lett.* **2015**, *17*, 4658. (c) Sharma, S.; Han, S. H.; Oh, Y.; Mishra, N. K.; Lee, S. H.; Oh, J. S.; Kim, I. S. *Org. Lett.* **2016**, *18*, 2568. (d) Sharma, S.; Han, S. H.; Jo, H.; Han, S.; Mishra, N. K.; Choi, M.; Jeong, T.; Park, J.; Kim, I. S. *Eur. J. Org. Chem.* **2016**, *2016*, 3611. For the C(sp³)-H functionalization using maleimides, see: (e) Han, S.; Park, J.; Kim, S.; Lee, S. H.; Sharma, S.; Mishra, N. K.; Jung, Y. H.; Kim, I. S. *Org. Lett.* **2016**, *18*, 4666.
- (10) (a) Luzzio, F. A.; Duveau, D. Y.; Lepper, E. R.; Figg, W. D. *J. Org. Chem.* **2005**, *70*, 10117. (b) Ishiyama, T.; Tokuda, K.; Ishibashi, T.; Ito, A.; Toma, S.; Ohno, Y. *Eur. J. Pharmacol.* **2007**, *572*, 160. (c) Deeks, E. D. *Drugs* **2015**, *75*, 1393.
- (11) (a) Shin, Y.; Han, S.; De, U.; Park, J.; Sharma, S.; Mishra, N. K.; Lee, E.-K.; Lee, Y.; Kim, H. S.; Kim, I. S. *J. Org. Chem.* **2014**, *79*, 9262. (b) Jeon, M.; Mishra, N. K.; De, U.; Sharma, S.; Oh, Y.; Choi, M.; Jo, H.; Sachan, R.; Kim, H. S.; Kim, I. S. *J. Org. Chem.* **2016**, *81*, 9878.
- (12) For the combination of Rh(III) or Ru(II) catalysts with PivOH for C-H functionalization, see: (a) Schipper, D. J.; Hutchinson, M.; Fagnou, K. *J. Am. Chem. Soc.* **2010**, *132*, 6910. (b) Hashimoto, Y.; Hirano, K.; Satoh, T.; Kakiuchi, F.; Miura, M. *Org. Lett.* **2012**, *14*, 2058.
- (13) Berridge, M. V.; Herst, P. M.; Tan, A. S. *Biotechnol. Annu. Rev.* **2005**, *11*, 127.
- (14) Skehan, P.; Storeng, R.; Scudiero, D.; Monks, A.; McMahon, J.; Vistica, D.; Warren, J. T.; Bokesch, H.; Kenney, S.; Boyd, M. R. *J. Natl. Cancer. Inst.* **1990**, *82*, 1107.
- (15) (a) Maiti, A. K. *Int. J. Cancer* **2012**, *130*, 1. (b) Valko, M.; Leibfritz, D.; Moncol, J.; Cronin, M. T.; Mazur, M.; Telser, J. *Int. J. Biochem. Cell Biol.* **2007**, *39*, 44.
- (16) (a) Zhang, X.; Wang, X.; Wu, T.; Li, B.; Liu, T.; Wang, R.; Liu, Q.; Liu, Z.; Gong, Y.; Shao, C. *Sci. Rep.* **2015**, *5*, 12579. (b) Zhang, F.; Lau, S. S.; Monks, T. J. *Toxicol. Sci.* **2011**, *120*, 87.